

Structural Analysis with Vibro-Acoustic Loads in LS-DYNA[®]

Mostafa Rassaian¹, Yun Huang², JungChuan Lee¹, Thomas T. Arakawa¹

¹Boeing Phantom Works Structures Technology – Advanced Analysis
Seattle, WA 98108, USA

²Livermore Software Technology Corporation
Livermore, CA 94551, USA

Abstract

Many structures are designed to operate in hot temperature and stringent aero-acoustic fatigue environment, e.g. the engine inlet and the heat shield of aircraft are subject to high temperature and sonic pressure level. It is important to evaluate the dynamic response of the structures exposed to both vibration and acoustic sources of excitations.

A new feature of structural analysis with vibro-acoustic loads has been implemented in LS-DYNA[®]. This feature is based on N-FEARA[®] finite element analysis tool developed by The Boeing Company. This new capability in LS-DYNA treats the structural response by finite element method coupled with acoustic field based on a known acoustic source behavior by spatial correlation function. The added capabilities enable the users to evaluate the response of structure to both base-excitation, or vibration and acoustic source in the frequency domain.

Various acoustic environments and sources of excitations can be considered, including base excitation defining random vibration, in addition to plane wave, progressive wave, reverberant wave, turbulent boundary layer, shock wave, representing various fields for acoustic sources of excitation. Modal acceleration method as well as modal superposition method is used to evaluate the dynamic behavior of structures in the frequency domain. The acceleration power spectral density (PSD) is defined in term of g^2/Hz used for vibration analysis. The input spectrum for the acoustic excitations can be either pressure PSD in psi^2/Hz or sound pressure level (SPL) in dB. For the latter, sound pressure level is first converted into pressure PSD. The coupling between the structures (represented by the modal shapes) and the acoustic excitations is expressed through the concept of joint acceptance. The results are presented in terms of PSD of the nodal displacements, velocities, accelerations, and element stresses, and the RMS (Root Mean Square) of those variables for a frequency range of interest.

Several efficient numerical techniques have been implemented to accelerate the solution phase, including the partition of the panel and subdivision of the range of frequencies. A restart option is provided in case users need to change the input acoustic spectrum or change the range of frequency in the output.

Furthermore, this novel feature of LS-DYNA provides users a method to replace an acoustic test environment by a shaker table test as a virtual qualification for testing method. This method is based on a conversion factor between the maximum of root mean square of displacement response due to acoustic pressure load and due to base acceleration load.

Several keywords have been introduced in LS-DYNA to facilitate this new feature. Numerical examples are given to demonstrate the new vibro-acoustic analysis capability which will be available in the next release of LS-DYNA.

1. Introduction

Many structures are designed to operate in hot temperature and stringent aero-acoustic fatigue environment, e.g. the engine inlet and the heat shield of aircraft are subject to high temperature and sonic pressure level. Overall sound levels of 150-170 dB are often encountered near turbojet

engines [1]. Sound levels over 185 dB have been estimated for the scram jet engines on advanced hypersonic aircraft [2]. It is important to evaluate the dynamic response of the structures exposed to both vibration and acoustic sources of excitations.

To model the behavior of structure under such high frequency sonic environment, Boeing Phantom Works has developed a finite element package N-FEARA, based on the mathematical formulation presented in section 3. The solution sequence was based on the implicit nonlinear finite element code – NIKE3D [3], which was developed in Lawrence Livermore National Laboratory. This tool has been successfully applied to evaluate hot aircraft structures to noise and vibration in addition to high cycle fatigue analysis of circuit board assemblies [4, 5]. Cross-validation between N-FEARA and Boeing's software SRA[®] (Sonic Response Analysis, which is based on MSC Nastran[®] and Patran[®]) was performed in [4].

The vibro-acoustic feature of the N-FEARA package has been implemented to LS-DYNA. It has provided LS-DYNA the new and unique capability of performing dynamic structural analysis with vibro-acoustic loads, including base-excitation, vibration and acoustic source in frequency domain.

This paper briefly documents the theory and the analysis procedure as relate to structural acoustic response for this new feature of LS-DYNA. Some examples are also given to demonstrate the reliability and capability of this new feature.

2. Description of the problem

The method considers a panel structure subjected to high frequency acoustic pressure, nodal force, base acceleration or random pressure excitation. The excitation environment is given in terms of PSD (power spectral density) values for a range of frequencies. The acoustic pressure can also be given in terms of SPL (sound pressure level) which can be transformed to PSD spectrum. In engineering practice, the input is given in the form of 1/3 octave band SPL in the field test. The output of the analysis is given in terms of PSD of displacement, acceleration, velocity for specified nodes, in addition to PSD of stress components for specified elements. The RMS (root mean square) of these values is also given, for a specified range of frequencies. The output helps to identify the location(s) with peak stress or strain for determining failure of the structure.

The analysis method is based on the coupling between the structures and the sonic excitation environment through the concept of joint acceptance function, where the structural dynamic behavior is characterized by its normal vibration modes.

3. Mathematical formulation

The acoustic pressure near surface of the structure is assumed to be known from the measurements taken in the field. Source of excitation includes base vibration and acoustic pressure. Response spectra computations are then carried out using the expressions developed for displacement, acceleration and stress PSD (power spectral density) response and RMS (root-mean-square) presented below. The detailed derivation can be found in [3].

PSD and RMS for displacement

Assuming linear beam theory, the general equation of motion is given by

$$\ddot{\eta}_i + 2\xi_i \omega_i \dot{\eta}_i + D(\eta_i) = \frac{1}{M_i} \int \phi_i(x) p(x, t) dx \quad (1)$$

where η_i is the modal deflection response at the i th degrees of freedom; M_i is the generalized mass; $\phi_i(x)$ is the mode shape; $p(x, t)$ is the pressure distribution at position x and time t , and $D(\cdot) = c^2 (\partial^2 \cdot / \partial x^2)^2$ with c being a constant. This equation represents a balance between inertial, elastic, damping and applied forces.

The complete solution for deflection response is then given by modal superposition method

$$y = \sum \phi_i(x) \eta_i(t) \quad (2)$$

which must satisfy the boundary conditions.

Taking Fourier transform on equation (1), the solution for the deflection response is obtained in frequency domain as

$$S_y(x, \omega) = \sum \phi_i(x) S_{\eta_i}(\omega) \quad (3)$$

The power spectrum is a real quantity defined by

$$W_y(x, \omega) = \frac{2}{T} S_y(x, \omega) S_y^*(x, \omega) \quad (4)$$

Where the asterisk indicates the complex conjugate and T is a time interval to be taken to the limit. Using the concept of Cross-correlation for pressure field, extending the equation (1) from a beam to a plate by replacing the points x and x' with position vectors \mathbf{r} and \mathbf{r}' respectively, and taking some necessary manipulation, one can write the displacement power spectral density response as

$$W_y(\mathbf{r}, \omega) = \frac{A^2 G(\omega)}{\omega^4} \sum_j \sum_m \frac{\phi_j(\mathbf{r}) \phi_m(\mathbf{r}) J_{jm}(\omega)}{|H_j(\omega)| |H_m(\omega)|} \quad (5)$$

Where

$$H_j(\omega) = (-1 + 2\xi_j \frac{\omega_j}{\omega} i + \frac{\omega_j^2}{\omega^2}) \quad (6)$$

M_j, M_m is the j th, and m th elements of generalized mass matrix.

$\phi_j(\mathbf{r})$ is the j th normal mode shape

$|\cdot|$ is the amplitude of complex variable

$G(\omega)$ is the reference PSD of sound pressure

$J_{jm}(\omega)$ is the joint acceptance which describes the coupling between an excitation pressure field and a structure represented by its normal vibration modes. $J_{jm}(\omega)$ is defined by

$$J_{jm}(\omega) = \frac{1}{A^2} \iint_{a \ a'} C(\mathbf{r}, \mathbf{r}', \omega) \phi_j(\mathbf{r}) \phi_m(\mathbf{r}') da da' \quad (7)$$

da, da' are infinitesimal area vectors and $C(\mathbf{r}, \mathbf{r}', \omega)$ is cross-power spectral density coefficient of the sound pressure level which is defined as

$$C(\mathbf{r}, \mathbf{r}', \omega) = \frac{W_p(\mathbf{r}, \mathbf{r}', \omega)}{G(\omega)} \quad (8)$$

$G(\omega)$ is PSD of a reference sound pressure. For homogeneous pressure fields,

$$C(\mathbf{r}, \mathbf{r}', \omega) = C(\mathbf{r} - \mathbf{r}', \omega) \quad (9)$$

For partially correlated and uncorrelated acoustic wave (plane wave, progressive wave, turbulent boundary layer), the cross-power spectral density coefficient can be expressed as

$$C(\xi, \eta, \omega) = G(\omega) \exp \left\{ -\frac{|\xi|}{\lambda_\xi(\omega)} - \frac{|\eta|}{\lambda_\eta(\omega)} - i \frac{\omega \xi}{U_\xi} - i \frac{\omega \eta}{U_\eta} \right\} \quad (10)$$

$$\xi = (\mathbf{r} - \mathbf{r}')|_x, \quad \eta = (\mathbf{r} - \mathbf{r}')|_y$$

$\lambda_\xi, \lambda_\eta$ is correlation scale along ξ and η

U_ξ, U_η is correlation scale along ξ and η

For reverberant wave, coherence function can be re-written as

$$C(\mathbf{r}, \omega) = G(\omega) \sin(k\mathbf{r}) / (k\mathbf{r}) \quad (11)$$

Where $\mathbf{r} = \xi \mathbf{i} + \eta \mathbf{j}$ and k is wave number $= \omega/c$.

For fully correlated acoustic wave, the cross-correlation function C is unity.

The input spectrum can be either pressure in psi^2/Hz or sound pressure level in dB. For the latter, sound pressure level is first converted into pressure following the formula

$$G(f) = 8.41 \times 10^{(SPL/10-18)} / \Delta f \quad (12)$$

Where $\Delta f = (2^{1/6} - 2^{-1/6})f_c$ for 1/3 octave band and $\Delta f = (2^{1/2} - 2^{-1/2})f_c$ for 1 octave band.

The RMS displacement is given by

$$u(\mathbf{r}) = \left(\int_{\omega_1}^{\omega_f} W_y(\mathbf{r}, \omega) d\omega \right)^{1/2} \quad (13)$$

PSD and RMS for acceleration

The PSD acceleration can be shown to follow the equation:

$$W_a(\mathbf{r}, \omega) = \omega^4 W_y(\mathbf{r}, \omega) = A^2 G(\omega) \sum_j \sum_m \frac{\phi_j(\mathbf{r}) \phi_m(\mathbf{r}) J_{jm}(\omega)}{M_j M_m |H_j(\omega)| |H_m(\omega)|} \quad (14)$$

The RMS acceleration is defined by:

$$a(\mathbf{r}) = \left(\int_{\omega_1}^{\omega_f} W_a(\mathbf{r}, \omega) d\omega \right)^{1/2} \quad (15)$$

PSD and RMS for stress

The stress response spectral density is determined by:

$$W_\sigma(\mathbf{r}, \omega) = \frac{A^2 G(\omega)}{\omega^4} \sum_j \sum_m \frac{\gamma_j(\mathbf{r}) \gamma_m(\mathbf{r}) J_{jm}(\omega)}{M_j M_m |H_j(\omega)| |H_m(\omega)|} \quad (16)$$

Where $\gamma_j(\mathbf{r})$ is stress coefficient at \mathbf{r} due to unit deflection of the j th mode stored in the j th column of the acceleration load transformation matrix.

The RMS stress is calculated by:

$$\sigma(\mathbf{r}) = \left(\int_{\omega_1}^{\omega_f} W_\sigma(\mathbf{r}, \omega) d\omega \right)^{1/2} \quad (17)$$

Other quantities such as velocity, acceleration, and strain were derived within the modal superposition framework for finite element method.

4. Some techniques to accelerate solution

Equation (7) involves double integration over surface. To reduce computational time, instead of performing the integration element by element, the area of integration is divided into a small number of sub-domains. The integration is then performed based on the few sub-partitions. LS-DYNA can perform the sub-partitioning based on the user provided number of sub-partitions in stream-wise and span-wise directions to achieve high accuracy. The partitioning scheme is based on the projection of the panel geometry onto a plane from which the partitioning algorithm subdivides the panel. This scheme works best when the structure is a flat (or nearly flat) panel and the plane (defined by three points on the panel) coincides with the plane of the structure. The partitioning method has been generalized for general curvilinear coordinate systems. For more details about the panel partitioning scheme, please refer to [3].

For broadband frequency analysis, sometimes it is impractical to cover the entire range in one run due to the limitation from the computer memory. To overcome this limitation, the frequency range of interest can be divided into subdivisions that numerical calculation can perform well in each sub-division. In principle each mode has effect for the whole range of frequency. In reality the response reaches the peak at its natural frequency and decay rapidly below and above the natural frequency. To accurately calculate the response, the frequency range should include an overlap for those slightly higher and lower than the range of each sub-division [3].

A restart feature is also implemented. This feature allows user to change the range of output frequency, or change the input acoustic or acceleration spectrum, after the first run, without re-performing the modal analysis for the structure.

5. Analysis process

This feature starts with modal analysis of the structures, which provides frequency, mode shape and mass matrix. If a preload from static pressure or temperature change is presumed, intermittent modal analysis is performed to incorporate the consideration of these preload effects on structural response. In case the results for stress components are requested, modal stress calculation is also performed, using the normalized modal shape deflection as the boundary conditions. Joint acceptance is computed based on the type of application (plane wave, reverberant wave, turbulent boundary layer, etc.) and the mode shapes. After that, the mode shape, joint acceptance and the given acoustic or acceleration spectrum are assembled to provide the final solution of PSD, RMS at nodes and elements and zero-cross frequency.

This feature also provides a method to convert an acoustic pressure PSD to a base acceleration PSD for a shaker-table test simulation [6]. The procedure can be illustrated as follows.

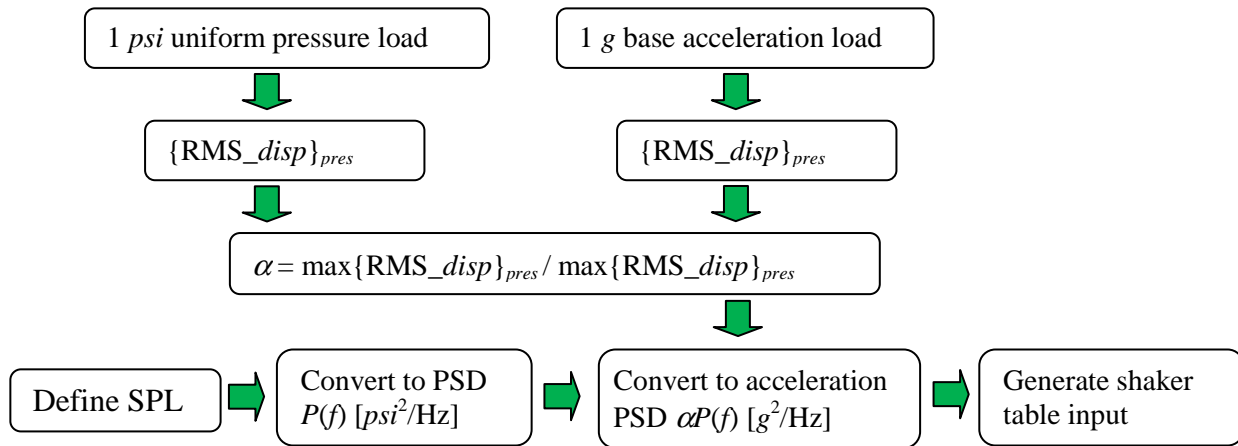


Figure 1. Conversion of acoustic input to shaker table input

With this method, one can easily replace the costly acoustic test with a rather inexpensive shaker table test.

6. Keywords

Several new keywords have been added to LS-DYNA to facilitate the vibro-acoustic analysis [7]. They are briefly introduced here.

*CONTROL_VIBRO_ACOUSTIC sets vibro-acoustic analysis control flags (e.g. the flag for stress analysis and restart) and defines the type of excitations; *LOAD_VIBRO-ACOUSTIC defines the acoustic spectrum load via a set of load curves and defines the area subjected to acoustic pressure; *DATABASE_POWER_SPECTRAL_DENSITY defines the location for PSD output; *DATABASE_POWER_SPECTRAL_DENSITY_FREQUENCY defines the range of frequencies for PSD output.

For a more detailed introduction of these keywords, please refer to the LS-DYNA Keyword User's Manual [7].

7. Examples

Several examples are included to illustrate the application of the new feature. For the purpose of validation, comparison to available results from other sources is included. Example 1 provides the structural response of a “L” shaped plate subjected to turbulent boundary layer, and compares the results with those given by N-FEARA; Example 2 discusses the effect of preload on the structural response with a plane wave environment, and a comparison of the results with SRA results is also given; Example 3 solves a real application of a Boeing engine inlet subjected to reverberant wave, and compares the results with those given by N-FEARA and SRA.

1) A “L” shaped plate subjected to turbulent boundary layer

The model analyzed is a 10”×10” L-Shape flat plate model consisting of 300 shell elements that is clamped along three edges (see Figure 3). The node 341 at the free-edge was selected as the evaluation point where the maximum acceleration (z) response occurs. A turbulent boundary

layer acoustic spectrum in the range of 31.5 Hz to 2000 Hz is used as input (the acoustic pressure is nearly constant with the value of 7E-03 psi²/Hz, the detailed loading data is in Appendix 1). The first 10 frequencies in modal analysis are employed. Solution was expanded to 10 modes or 2500Hz, whichever occurred first.

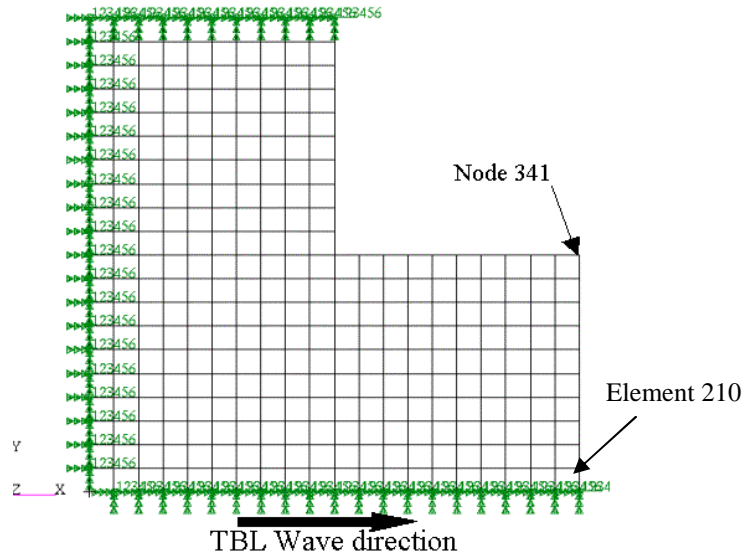


Figure 2. a L-Shape flat plate subjected to TBL wave

The z-velocity and z-acceleration results given by LS-DYNA and by N-FEARA are compared in Table 1. The results are given at node 341. Table 1 shows the PSD values of the velocity and acceleration for the first 10 output frequencies.

Freq (Hz)	PSD of z-velocity (in ² /s ² /Hz)		PSD of z-acceleration (g ² /Hz)	
	LS-DYNA	N-FEARA	LS-DYNA	N-FEARA
31	1.8809E-01	1.8784E-01	4.7893E-02	4.7829E-02
32	2.0067E-01	2.0040E-01	5.4446E-02	5.4373E-02
33	2.1368E-01	2.1340E-01	6.1657E-02	6.1574E-02
34	2.2713E-01	2.2683E-01	6.9570E-02	6.9477E-02
35	2.4102E-01	2.4070E-01	7.8231E-02	7.8126E-02
36	2.5536E-01	2.5501E-01	8.7687E-02	8.7570E-02
37	2.7014E-01	2.6977E-01	9.7988E-02	9.7856E-02
38	2.8537E-01	2.8498E-01	1.0918E-01	1.0904 E-01
39	3.0105E-01	3.0065E-01	1.2133E-01	1.2116 E-01
40	3.1720 E-01	3.1677E-01	1.3447E-01	1.3429E-01

Table 1: PSD of z-velocity and z-acceleration at node 341

The distribution of RMS displacement and Von mises stress can be found in Figure 3 and Figure 4. In Figure 4, the Von mises stress employs the maximum value at the three integration points through thickness.

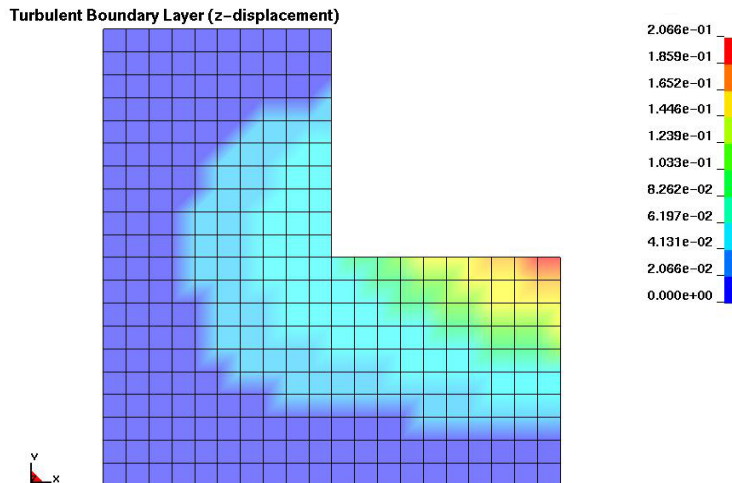


Figure 3. RMS of z-displacement for the L-shape plate (unit: inch)

One can see that the maximum value of the RMS z-displacement happens at node 341.

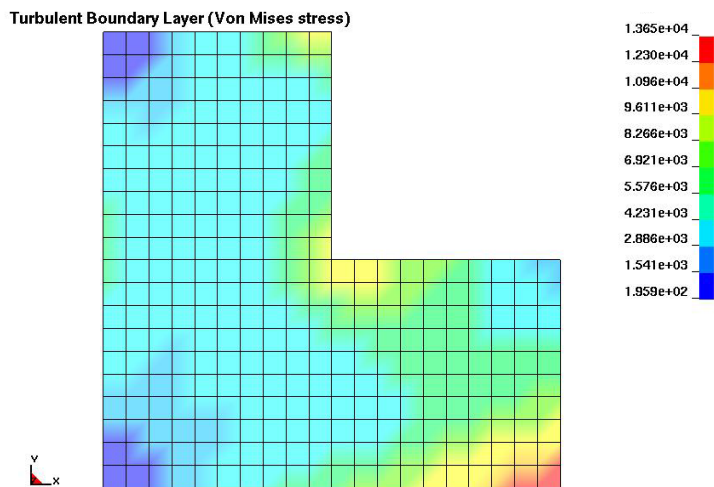


Figure 4. RMS of Von mises stress for the L-shape plate (unit: psi)

The maximum RMS of Von mises stress happens at the lower-right corner (element 210) where the free edge joins the clamped edge.

2) Effect of preload on the vibro-acoustic response

There are many applications where one has to account for thermal or pressure preload coupled with sonic environment [8]. The thermal preload comes from temperature difference from its neutral temperature. Typically the most severe acoustic or vibration environment occurs when the structure is under static preload. Changes in geometry, stress, material, and contact conditions will affect the eigenvalues and mode shape. In LS-DYNA, there are several ways to account for preload effect. For example, one can use the keyword `*INITIAL_STRESS_SHELL`, `*INITIAL_STRESS_SECTION`, etc. Here we use a method based on the intermittent eigenvalue analysis. For this purpose, one needs to use `NEIG=-LCID` in the keyword `*CONTROL_IMPLICIT_EIGENVALUE` where `LCID` is the curve ID, which indicates when to extract eigenvalues, and how many to extract [7].

The same problem in example 1) is re-considered here, for case (1) no preload; and case (2) with 8psi pressure preload applied on the panel surface. Due to the nature of boundary condition and load, the panel undergoes both out-of-plane as well as in-plane deformations in case (2).

Table 2 compares the frequencies given by LS-DYNA and SRA (based on MSC Nastran), for case (1) and case (2) for the first seven modes. A plane wave acoustic environment is assumed for this example (the loading spectrum is in Appendix 2).

Mode No.	case (1) no preload		case (2) with 8psi preload	
	LS-DYNA	SRA	LS-DYNA	SRA
1	3.0960E+02	3.0661E+02	4.2213E+02	4.1809E+02
2	5.8821E+02	5.8016E+02	8.0691E+02	8.0090E+02
3	1.0822E+03	1.0690E+03	1.2563E+03	1.2435E+03
4	1.2697E+03	1.2534E+03	1.3974E+03	1.3819E+03
5	1.5282E+03	1.5066E+03	1.6006E+03	1.5789E+03
6	1.9244E+03	1.8940E+03	2.0494E+03	2.0191E+03
7	2.0749E+03	2.0365E+03	2.2705E+03	2.2325E+03

Table 2. Frequencies without preload and with 8psi preload (unit: Hz)

One can see that the differential stiffness effects cause the panel to appear “stiffer” than case (1) no preload. For example, the first mode frequency increased from 310 Hz to 422 Hz, the second mode increased from 588 Hz to 807 Hz. A similar trend also exists at the higher modes.

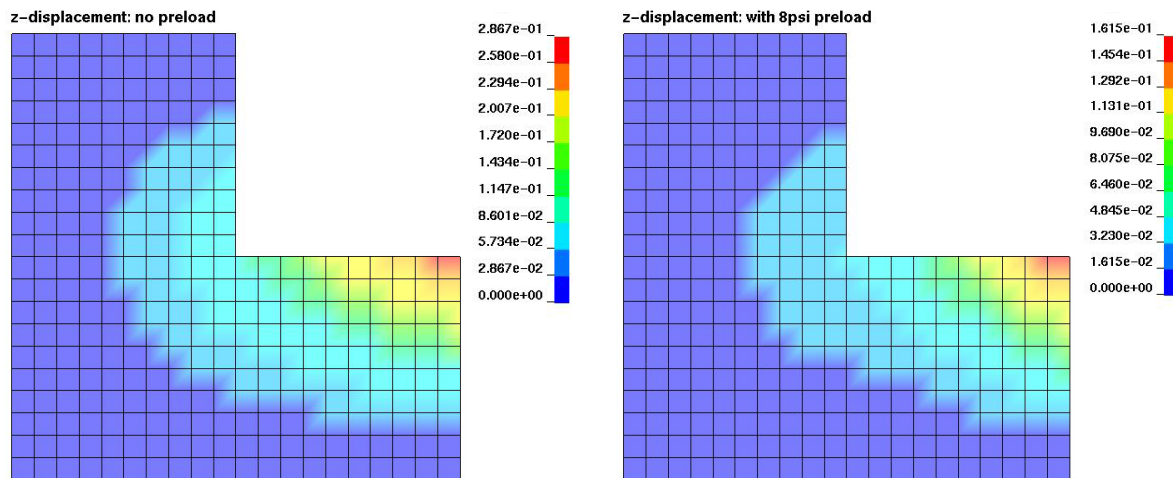


Figure 5. RMS of z-displacement for plane wave for cases (1) and (2) (unit: inch)

Figure 5 shows the RMS z-displacement plots for the panel for case (1) without preload and case (2) with 8psi preload; similar plots for RMS z-acceleration can be found in Figure 6.

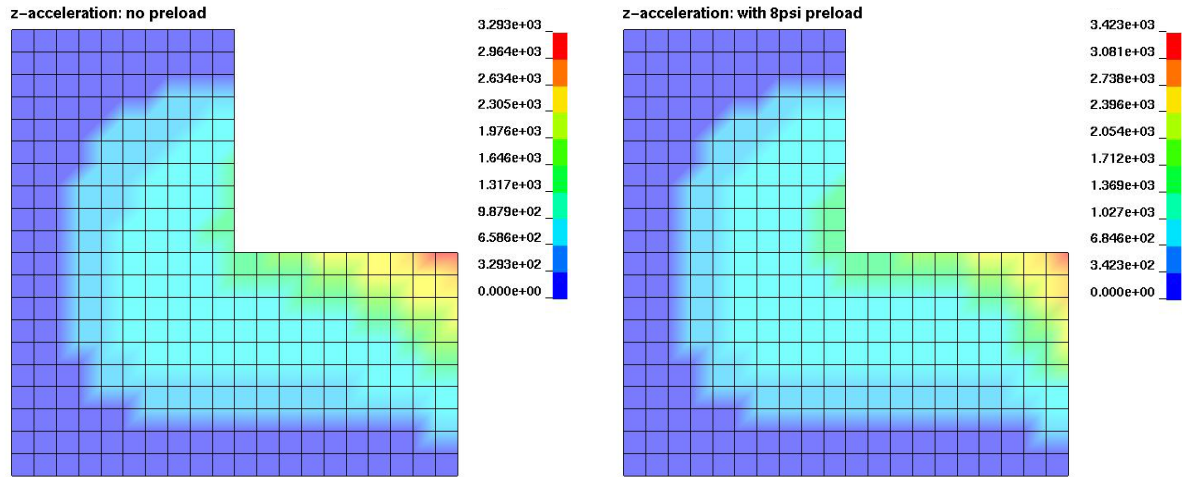


Figure 6. RMS of z-acceleration for plane wave for cases (1) and (2) (unit: g)

Figures 7 and 8 show the RMS Von mises stress plots for the two cases at the upper and lower surfaces respectively.

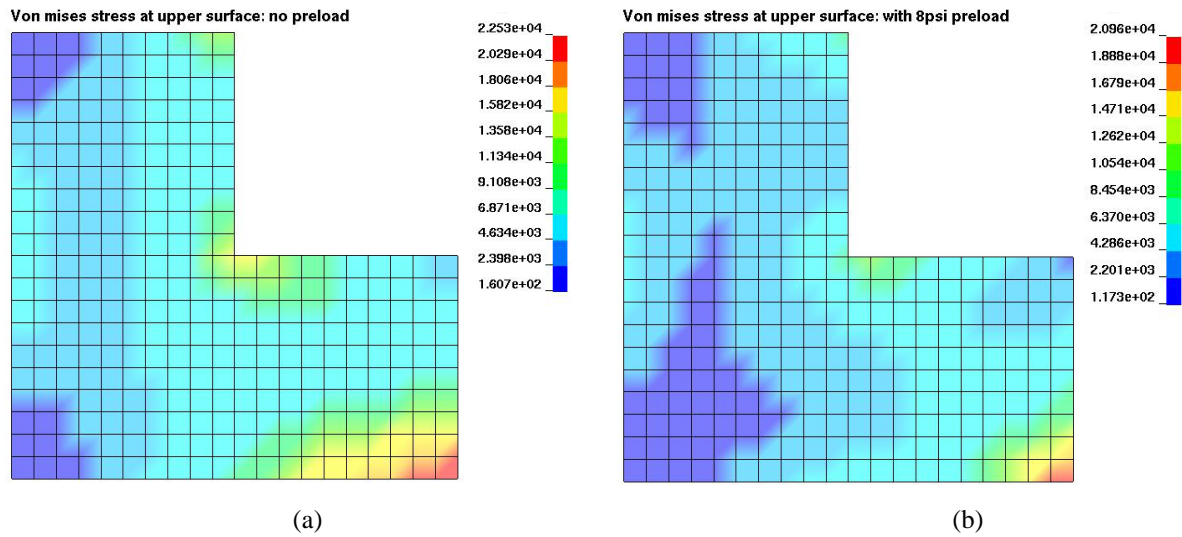


Figure 7. RMS of Von mises stress at upper surface for plane wave for cases (1) and (2) (unit: psi)

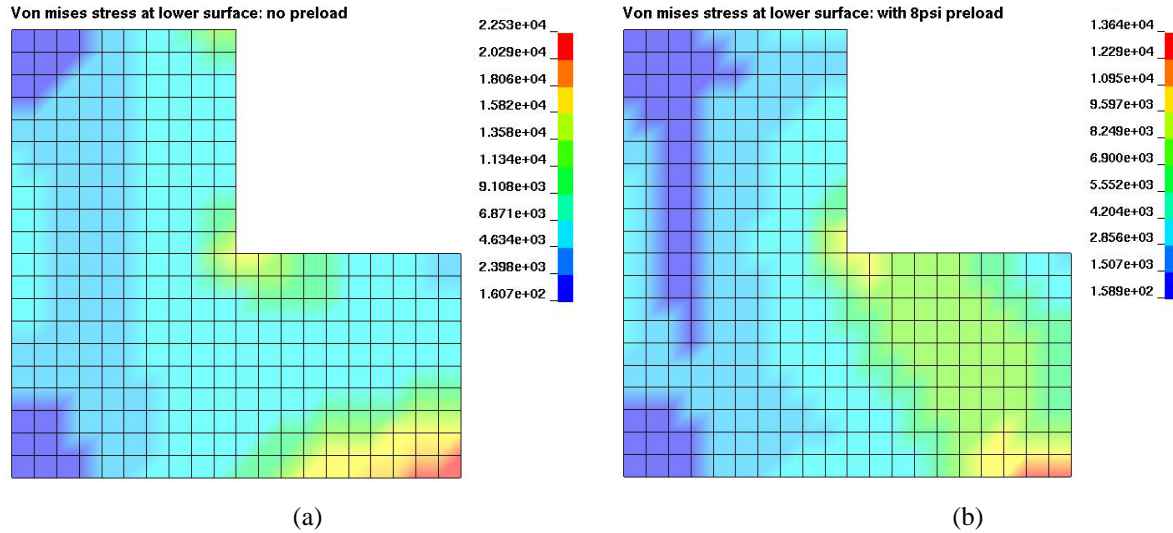


Figure 8. RMS of Von mises stress at lower surface for plane wave for cases (1) and (2) (unit: psi)

It can be seen that the displacement and stress with preload is much smaller compared with the displacement and stress response without preload. The maximum of RMS of z-displacement decreases from 0.2867 inch for the case of no preload to 0.1615 inch for the case of 8psi preload. At the upper surface, the maximum of RMS of Von mises stress decreases from 22530 psi for the case of no preload to 20960 psi for the case of 8psi preload. At the lower surface, the maximum of RMS of Von mises stress decreases from 22530 psi for the case of no preload to 13640 psi for the case of 8psi preload. Acceleration behaves differently in that there is no significant difference between the cases with and without preload. This finding is in agreement with Rassaian and Lee using N-FEARA [3, 8]. The distributions of displacement and acceleration for the panel with 8psi preload are very similar to those without preload. For example, the maximum of RMS of z-displacement and z-acceleration appear at node 341, for both cases of without preload and with 8psi preload. This is due to the same boundary condition used in the two cases.

We also noticed that the distributions of the RMS of Von mises stress at the upper and lower surface are same for case (1) (see Figure 7 (a) and Figure 8 (a)). On the other hand, Figure 7 (b) and Figure 8 (b) demonstrates the influence of preload by inducing in-plane stress accompanied by bending stress leading to two quite different stress distributions on the upper and lower surfaces. For example, a 20960 psi maximum Von mises stress at the upper surface is compared to 13640 psi at the lower surface due to the static preload. In both cases, the maximum of RMS of Von mises stress appear at the lower-right corner (element 210).

The results given by LS-DYNA match well with those by SRA. A list of corresponding maximum values by LS-DYNA and SRA is given in Table 3.

RMS values	case (1) no preload		case (2) 8psi preload	
	LS-DYNA	SRA	LS-DYNA	SRA
z-displacement (inch)	2.867E-1	2.87E-1	1.615E-1	1.63E-1
z- acceleration (g)	3.293E+3	3.288E+3	3.423E+3	3.418E+3
Von mises stress at upper surface (psi)	2.253E+4	2.23E+4	2.096E+4	1.97E+4
Von mises stress at lower surface (psi)	2.253E+4	2.23E+4	1.364E+4	1.39E+4

Table 3. Maximum RMS values by LS-DYNA and SRA

Figures 9 and 10 show the Von mises stress at the upper surface for case (1) and case (2) by SRA. Comparing the two figures with Figure 7, one can find that the distributions of the stress are very similar to those given by LS-DYNA.

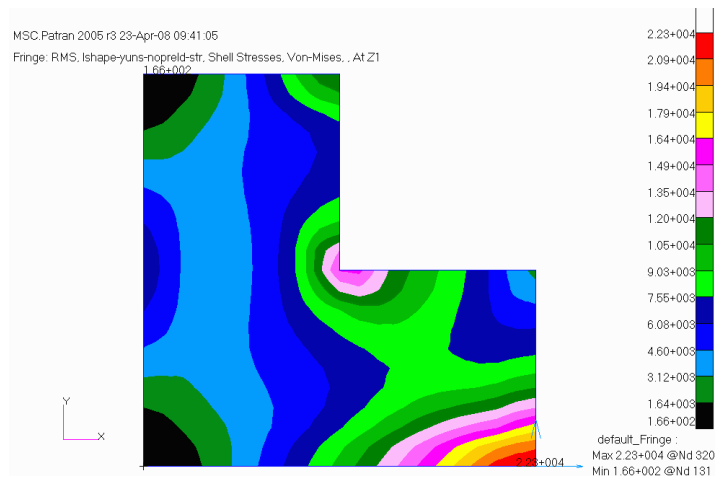


Figure 9: RMS of Von mises stress at upper surface for cases (1) by SRA (unit: psi)



Figure 10: RMS of Von mises stress at upper surface for cases (2) by SRA (unit: psi)

3) Boeing engine inlet problem

The finite element model of a Boeing engine inlet design study is given in Figure 11. This example is the lap-joint model of a highly-curved inlet consisted of the leading edge ‘lip’ region which transitions to a composite section via a joint just aft of the forward bulkhead. The problem is more complicated than the previous two due to a wider range of geometric, material and loading conditions unique to this problem, e.g., structures with tightly curved vs. near flat load bearing surfaces. SPF titanium technology was considered for the engine inlet for savings in manufacturing and life cycle costs. The key question to address is the durability of the forward bulkhead – in particular at its juncture with the inner and outer barrel segments under the vibro-acoustic loading of the ambient noise environment.

To take advantage of the symmetry condition under symmetric loading, only a quarter of the full model is considered. The quarter model is composed with 11 material models; 4600 nodes; 1440 solid elements and 4434 shell elements. The structural behavior of this complex structure is

studied under a reverberant wave acoustic environment. The PSD and RMS of displacement, acceleration and stress level and the consequent threat to structural life based on the high cycle fatigue considerations is assessed. The reverberant wave input load were derived from the 1/3 octave band data, see Appendix 3.

The analysis was solved for the first 100 modes, using 3% critical damping.

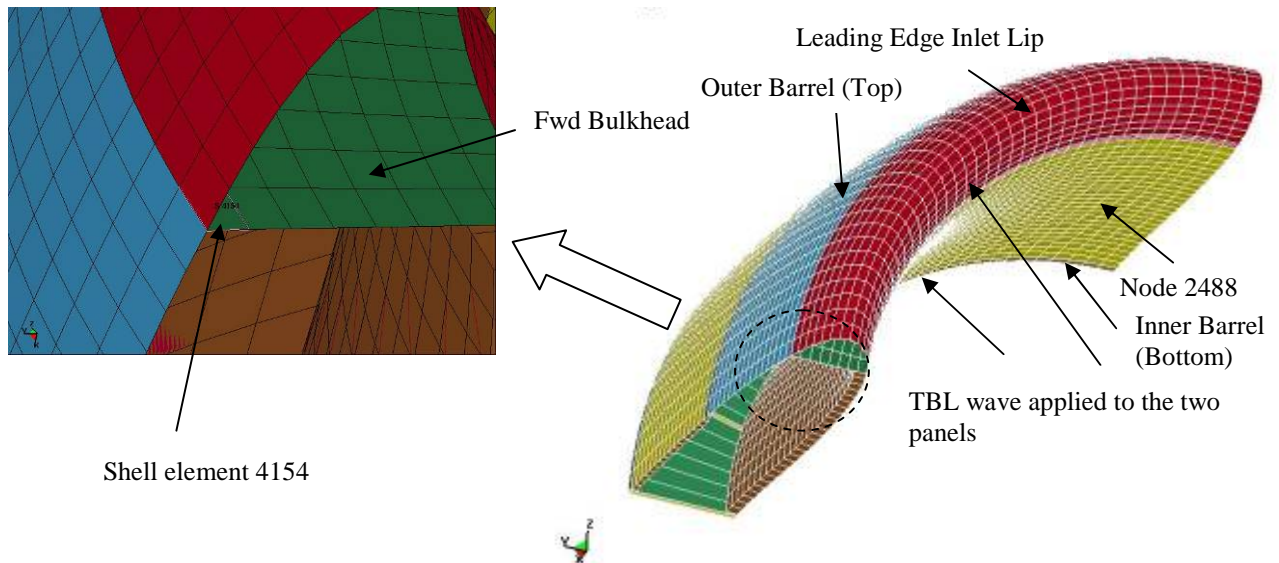


Figure 11. Boeing inlet finite element model

This problem was solved by LS-DYNA, N-FEARA and SRA separately.

Table 4 shows the first 10 natural frequencies obtained with LS-DYNA, N-FEARA and SRA. Note that SRA used a full model since it was used for a plane wave analysis and this type of analysis is not computationally intensive.

Mode No.	LS-DYNA (quarter model)	N-FEARA (quarter model)	SRA (full model)
1	2.8461E+01	2.8671E+01	3.3888E+01
2	9.0344E+01	9.0913E+01	7.2637E+01
3	9.2587E+01	9.3230E+01	7.2644E+01
4	9.3438E+01	9.4150E+01	8.4199E+01
5	9.5900E+01	9.6577E+01	8.4298E+01
6	9.9389E+01	9.9982E+01	1.1829E+02
7	1.0383E+02	1.0434E+02	1.1903E+02
8	1.0708E+02	1.0976E+02	1.2420E+02
9	1.0936E+02	1.1601E+02	1.2580E+02
10	1.1617E+02	1.1644E+02	1.2707E+02

Table 4. The first 10 Natural frequencies (unit: Hz)

The PSD value of velocity and stress at two observation locations (node 2488 and shell element 4154) is compared in Figure 12 and Figure 13.

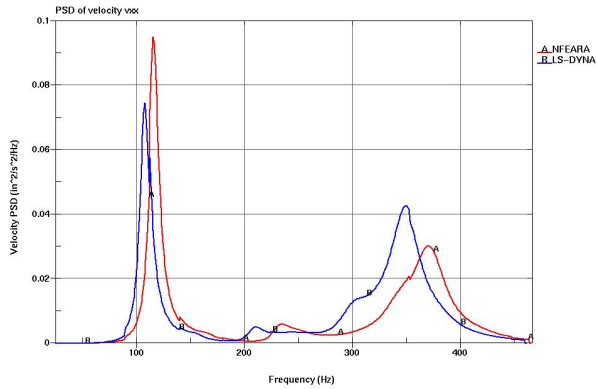
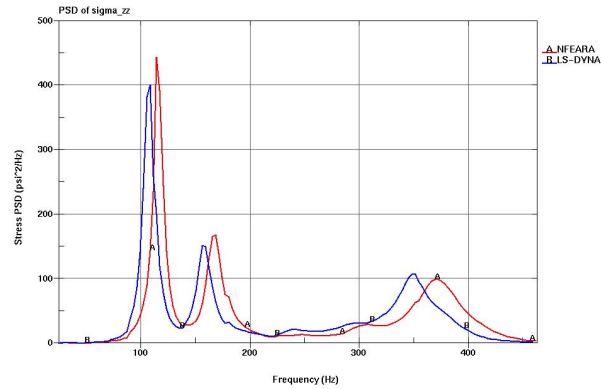
Figure 12. PSD of v_x at node 2488 (unit: $\text{in}^2/\text{s}^2/\text{Hz}$)Figure 13. PSD of σ_{zz} at element 4154 (unit: psi^2/Hz)

Figure 14 shows the RMS of Von mises stress (maximum of the value at three integration points through thickness) for the quarter model.

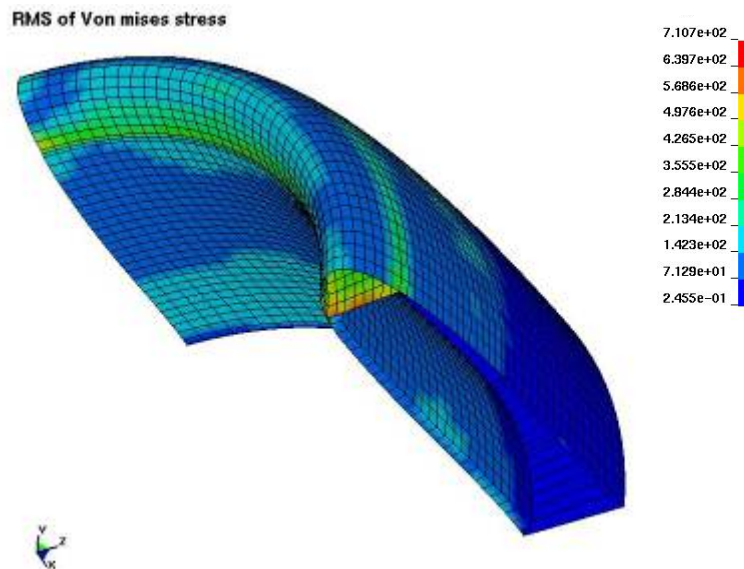


Figure 14. RMS of Von mises stress of the quarter model

The results are generally in reasonable agreement. Table 4 shows that the natural frequencies obtained with LS-DYNA are very close to those obtained with N-FEARA, and are also close to the results given by SRA (based on MSC Nastran). The distribution and magnitude of the RMS of Von mises stress is also in agreement with N-FEARA and SRA [4]. For example, in the results given by each of the three tools, the maximum RMS of Von mises stress happens on the edge of the forward bulkhead section. The maximum RMS of Von mises stress at integration points provided by LS-DYNA is 710.7 psi which compares to 832 psi by N-FEARA. The maximum RMS of Von mises stress at average over an element is 599.8 psi by LS-DYNA which compares to 585 psi by N-FEARA. The stress imposed by the reverberant loading is below the allowable and poses no threat to the structure in this area. The minor discrepancy between the results may come from the different element formulations employed in the three different softwares. For example, N-FEARA used B-bar solid element and Hughes-Liu shell element, while LS-DYNA used constant stress solid element and fully integrated shell element; Meanwhile SRA used anisotropic composite material properties for shell elements while in N-

FEARA and LS-DYNA the averaged (or ‘smeared’) isotropic properties were used [4]. This may be another reason for the discrepancy between the results by SRA and by the other two software.

8. Conclusion

A vibro-acoustic analysis feature has been implemented to LS-DYNA, based on Boeing software N-FEARA, a NIKE3D-based finite element tool for structural analysis of vibro-acoustic loads. N-FEARA is computationally efficient and powerful but intended for use by analysts familiarized with NIKE3D [5]. With the implementation of N-FEARA module into LS-DYNA, the vibro-acoustic structural analysis feature can be accessed by the masses. Several new keywords have been introduced in LS-DYNA to facilitate the use of this feature. Several case studies were performed to validate the implementation and demonstrate the new capability. The results obtained with LS-DYNA are in reasonable agreement with those given by N-FEARA and SRA.

The future development of this feature includes: MPP implementation; visualization through LS-PREPOST®; validation for more complicated applications and direct comparison with experimental data.

References

1. Blevins R.D. An approximate method for sonic fatigue analysis of plates and shells. *Journal of Sound and Vibration* 129(1): 51-71, 1989.
2. Roussos L.A., Mixson J. S. NASA Technical Memorandum 89143, Langley Research Center, Hampton, Virginia, April 1987. *Acoustic fatigue: overview of activities at NASA Langley*.
3. Rassaian M., Lee J. N-FEARA – NIKE3D-based FE tool for structural analysis of vibro-acoustic loads. *Boeing technical report*, 9350N-GKY-02-036, 2003.
4. Arakawa T., Lee J. and Rassaian M. Phantom Works Acoustic Analysis Tools SRA and N-FEARA Enhancements using Engine Inlet to Reverberant Wave Problem. *Boeing technical report*, 975EN-GKY-04-030, 2004.
5. Glenn G., Rassaian M., Laminar Flow Inlet Acoustic Analysis for the Extended Joint Concept. *Boeing technical report*, 975EN-GKY-04-020, 2004.
6. Rassaian M., Lee J., Young G.K., Landmann A.E. Acoustic pressure load conversion method to vibration spectra. *United States Patent* 6363789, publication 2002.
7. LS-DYNA® Keyword User’s Manual. Version 971. Livermore Software Technology Corporation, 2007.
8. Rassaian M. Preload Effect in Finite Element Modeling of Vibration/Acoustic Response of Structures. *Boeing technical report*.

Appendix

Appendix 1. Turbulent Boundary Layer Load Spectrum for Example 1.

Freq (Hz)	Acoustic pressure (psi ² /Hz)	Phase velocity	Exponential Decay in Flow-wise Direction	Exponential Decay in Span-wise Direction
31.5	7.049E-03	3.497E+03	2.613	3.885E-01
40	7.049E-03	3.668E+03	2.616	3.888E-01
50	7.049E-03	3.836E+03	2.619	3.892E-01
63	7.049E-03	4.017E+03	2.625	3.899E-01
80	7.049E-03	4.214E+03	2.634	3.910E-01
100	7.048E-03	4.406E+03	2.648	3.926E-01
125	7.047E-03	4.607E+03	2.670	3.951E-01
160	7.046E-03	4.840E+03	2.708	3.995E-01
200	7.044E-03	5.061E+03	2.762	4.058E-01

250	7.041E-03	5.292E+03	2.843	4.155E-01
315	7.036E-03	5.542E+03	2.971	4.306E-01
400	7.029E-03	5.814E+03	3.168	4.540E-01
500	7.017E-03	6.079E+03	3.430	4.855E-01
630	6.998E-03	6.366E+03	3.799	5.300E-01
800	6.967E-03	6.676E+03	4.283	5.884E-01
1000	6.922E-03	6.976E+03	4.788	6.486E-01
1250	6.855E-03	7.283E+03	5.232	6.998E-01
1600	6.741E-03	7.617E+03	5.448	7.199E-01
2000	6.590E-03	7.887E+03	5.254	6.887E-01

Appendix 2. Plane Wave Load Spectrum for Example 2.

Freq (Hz)	SPL (dB)
50	155.7
63	156.7
80	157.7
100	158.7
125	159.7
160	160.7
200	161.7
250	162.7
315	162.7
400	162.7
500	162.7
630	162.7
800	162.7
1000	162.7
1250	161.6
1600	160.5
2000	159.3

Appendix 3. Reverberant Wave Load Spectrum for Example 3.

Freq (Hz)	SPL (dB)	Phase velocity	Exponential Decay in Flow-wise Direction	Exponential Decay in Span-wise Direction
25	126	4.330E+03	3.242	0.666
31.5	126	4.330E+03	3.242	0.666
40	126	4.330E+03	3.242	0.666
50	126	4.330E+03	3.242	0.666
63	129.7	4.535 E+03	3.251	0.666
80	132.9	4.757 E+03	3.266	0.667
100	135.9	4.974 E+03	3.287	0.669
125	138.2	5.201 E+03	3.321	0.671
160	140.2	5.464 E+03	3.380	0.676
200	142.2	5.713 E+03	3.462	0.682
250	143.9	5.974 E+03	3.587	0.691
315	144.8	6.257 E+03	3.779	0.706
400	145.6	6.563 E+03	4.070	0.729
500	145.9	6.862 E+03	4.451	0.760